

# Modelling dynamics of undetectable disease in leukemia concerning therapy

A FINAL-YEAR THESIS

Submitted to  
Indian Institute of Science Education and Research Pune  
in partial fulfillment of the requirements for the  
BS-MS Dual Degree Programme

by

Saumil Shah  
(20151179)

Supervised by  
Prof. Dr. Arne Traulsen  
Max Planck Institute for Evolutionary Biology, Ploen, Germany



Indian Institute of Science Education and Research Pune  
Dr. Homi Bhabha Road, Pashan, Pune 411008, INDIA

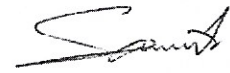
May, 2020

© Saumil Shah 2020  
All rights reserved

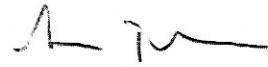


# Certificate

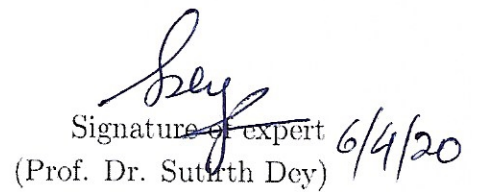
This is to certify that this thesis entitled “Modelling dynamics of undetectable disease in leukemia concerning therapy” towards the partial fulfilment of the BS-MS dual degree programme at the Indian Institute of Science Education and Research, Pune represents study/work carried out by Saumil Shah at the Max Planck Institute for Evolutionary Biology, Ploen, Germany, under the supervision of Prof. Dr. Arne Traulsen, Director, Evolutionary Theory, during the academic year 2019 - 2020.



Signature of candidate  
(Saumil Shah)



Signature of supervisor  
(Prof. Dr. Arne Traulsen)



Signature of expert 6/4/20  
(Prof. Dr. Sutrith Dey)

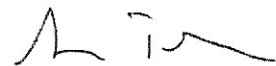


# Declaration

I hereby declare that the matter embodied in the report entitled “Modelling dynamics of undetectable disease in leukemia concerning therapy” are the results of the work carried out by me at the Department of Evolutionary Theory, Max Planck Institute for Evolutionary Biology, Ploen, Germany, under the supervision of Prof. Dr. Arne Traulsen and the same has not been submitted elsewhere for any other degree.



Signature of candidate  
(Saumil Shah)



Signature of supervisor  
(Prof. Dr. Arne Traulsen)



Signature of expert  
(Prof. Dr. Sutirth Dey)



# Acknowledgments

I wish to express foremost gratitude to my supervisor, Prof. Dr. Arne Traulsen, for granting me the exceptional opportunity to carry out my final-year project in his group. He consistently allowed this project to be my own work but steered me in the right direction whenever he thought I needed it. I feel not only fortunate but also honored to be a part of the diverse and adept department he has put together.

My sincere thanks go to Prof. Dr. Sutirth Dey for offering me the opportunity to work on diverse and exciting projects in his lab. His presence had a crucial contribution to the start of my interdisciplinary journey. The Population Biology Lab has been like a family and will always hold a special spot.

I want to record my appreciation for Dr. Michael Raatz, my mentor during the final-year, for his understanding, encouragement, and personal attention. His doors were always open for my most naive concerns, sometimes outside the working hours.

I am indebted to Dr. Yashraj Chavhan, my mentor in Population Biology Lab, for all the fruitful discussions, and tutoring to the most delicate details.

The facilities and the financial support provided by the Max Planck Institute of Evolutionary Biology are sincerely appreciated, without which this project couldn't have been possible.

I want to recognize Dr. Vineeta Bal and Dr. Satyajit Rath for providing the most indispensable courses, covering far beyond just the classrooms.

I thank my colleagues in the Evolutionary Theory department and the Population Biology lab for the stimulating discussions, and all the fun we had.

I want to thank all my friends at the Indian Institute of Science Education and Research for making the five-year journey memorable.

Finally, I must express my very profound gratitude to my parents and to my sister for providing unbounded love and comprehensive support in all my endeavors. I thank Disha, as well, for making me feel homely from the moment I arrived on a new continent.





# Contents

<b>1</b>	<b>Introduction</b>	<b>1</b>
1.1	Blood . . . . .	1
1.2	Acute Lymphoblastic Leukemia . . . . .	2
1.3	Current Treatment . . . . .	3
1.4	Recent Achievements . . . . .	3
1.5	Literature Survey . . . . .	4
1.6	Scope of this study . . . . .	5
1.7	Objectives . . . . .	6
<b>2</b>	<b>Methods</b>	<b>7</b>
2.1	Outline . . . . .	7
2.2	Reactions . . . . .	8
2.3	Master Equation . . . . .	8
2.4	Diffusion Approximation . . . . .	9
2.5	The Fokker-Planck Equation . . . . .	10
2.6	Mean-field Limit . . . . .	11
2.7	Stochastic Model . . . . .	11
2.8	First-passage Analysis . . . . .	12
2.9	Probability of First-exit . . . . .	13
2.10	Mean First-exit Time . . . . .	14
2.11	Numerical Solutions . . . . .	16
<b>3</b>	<b>Model for Chemotherapy</b>	<b>17</b>
3.1	Master Equation . . . . .	18
3.2	Fokker-Planck Equation . . . . .	19
3.3	Mean-field Limit . . . . .	19
3.4	Stochastic Model . . . . .	22
3.5	First-passage Analysis . . . . .	22
<b>4</b>	<b>Model for Immunotherapy</b>	<b>25</b>
4.1	Master Equation . . . . .	27
4.2	Fokker-Planck Equation . . . . .	27
4.3	Mean-field Model . . . . .	28
4.4	Stochastic Model . . . . .	30
4.5	First-passage Analysis . . . . .	31
<b>5</b>	<b>Discussion</b>	<b>33</b>
	<b>References</b>	<b>37</b>



# List of Tables

3.1	Symbols: chemotherapy . . . . .	17
3.2	Reactions: chemotherapy model . . . . .	18
4.1	Symbols: immunotherapy . . . . .	25
4.2	Reactions: immunotherapy model . . . . .	26



# List of Figures

1.1	Hematopoietic cell lineage . . . . .	2
1.2	Immunotherapy: Blinatumomab . . . . .	4
2.1	Flux created by reactions . . . . .	9
3.1	Illustration: chemotherapy model . . . . .	18
3.2	Disease dynamics in chemotherapy . . . . .	21
3.3	Comparison of different boundary sizes . . . . .	23
3.4	Comparison of deterministic and stochastic dynamics. . . . .	23
4.1	Illustration: immunotherapy model . . . . .	26
4.2	Phase portraits of immunotherapy . . . . .	29
4.3	Exit probabilities under immunotherapy . . . . .	32



# Abstract

The recent developments in antibody-based immunotherapy are believed to be promising against B cell leukemia, the most commonly diagnosed blood cancer. This disease has a peculiar tendency to reappear and lacks a quantitative understanding of post-treatment residual disease, which may have a role in the relapse. The need to predict the relapse, and reduce the adverse toxic effect of current standard, chemotherapy, demands a quantitative effort. We formulate a stochastic model that captures not only the deterministic behavior but also the fluctuations taking place in the residual disease. We also use first-passage analysis techniques developed for random walks to predict the long-term effects of fluctuations. The immunotherapy model predicts the containment of tumors for an adequate response of the immune system. We propose a sequential chemotherapy-immunotherapy strategy that may provide better outcomes. The mathematical workflow developed here sheds light on an equivalent formulation of master equations, that provides remarkable speed up for numerical computations. All in all, we provide a cell-population based stochastic model, to understand contemporary leukemia treatments, that can be used to test strategies as well as their outcomes.





# Chapter 1

## Introduction

### 1.1 Blood

Every living cell in our body depends on blood for its normal working. Blood is a fluid tissue that maintains the physio-chemical environment for cells within the functional limits throughout the body. The blood continually circulates in the body delivering oxygen, nutrients, and other vital substances while providing means for excretion of cellular metabolic waste and carbon dioxide. Blood is a heterogenous fluid comprised of plasma and blood cells. Plasma is a slightly yellow clear fluid that contains essential substances in the form of solution or suspension. Blood cells are divided into three types based on their morphology and function: platelets, red blood cells (RBC), and white blood cells (WBC). The platelets are responsible for clotting of blood on the damaged surface while the RBCs carry oxygen to the cells.

The WBCs share a crucial role in the immune system of our bodies. There are two sub-types in the immune system: innate system and adaptive system. The adaptive immune system is comprised of highly specialized cells that can identify foreign objects and eliminate them. The lymphocytes, namely, B cells and T cells are vital players of the adaptive immune system. The B cells can manufacture antibodies (protein macromolecule), specific to pathogens, that neutralize and help to kill the pathogens. The T cells can command B cells and several other cells that can perform mass killing of disease-causing microbes. T lymphocytes can also command our abnormal cells to commit suicide; due to this effector function, this specialized subset is known as the killer T cells.

## 1.2 Acute Lymphoblastic Leukemia

A cell, within a multicellular lifeform, matures from a single zygote cell to a complex system of tissues, or to cells performing different tasks. The body keeps a reservoir of unmaturing stem cells as most of the mature cells lose their ability to divide. The specialization of different cells is acquired through a process called cellular differentiation. All the blood cells in the circulation are differentiated from hematopoietic stem cells (HSC) of the bone marrow (Figure 1.1). The stem cells, for a protective reason, do not divide themselves but give rise to progenitor cells that undergo proliferation and differentiation. The B and T lymphocytes are differentiated from a lymphoid progenitor through multiple steps of differentiation.

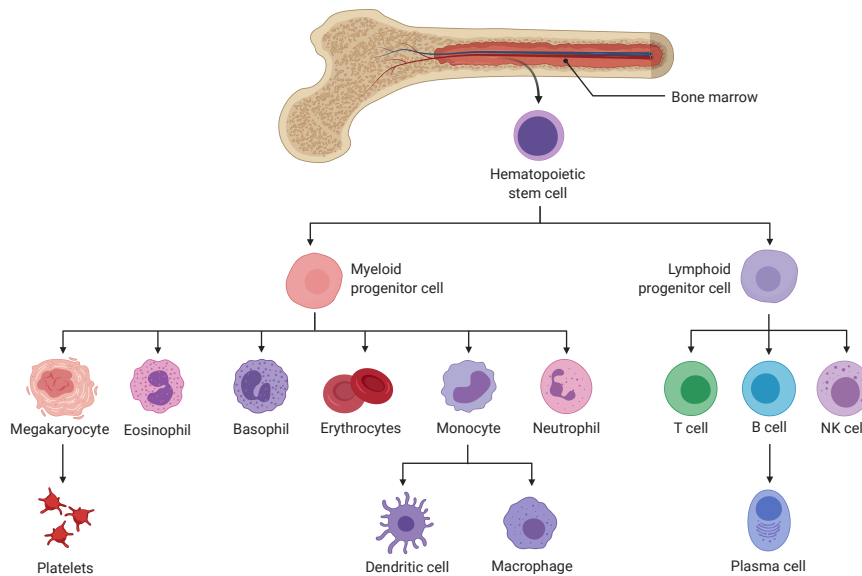


Figure 1.1: **The hierarchy of hematopoietic cell lineage.** The hematopoietic stem cells differentiate into myeloid and lymphoid progenitor cells; these progenitors give rise to the myelocytes and lymphocytes, respectively. B cells and T cells, which make up the adaptive immune system are small lymphocytes differentiated from the lymphoid progenitor cells.

Leukemia is a group of disorders of cell proliferation, and differentiation arrest in the blood cells. The accumulation of a series of genetic modifications in hematopoietic progenitors may lead to leukemia. Acute lymphoblastic leukemia (ALL) is a malignant disorder of lymphoid precursors due to specific genetic modifications (Pui et al. 2008). ALL is the most common form of cancer among children between the age of 2 and 5. It is also the most diagnosed form of leukemia in adults after the age of 50 (Faderl et al. 2010). WBC count in a healthy individual typically does not exceed  $10^4$  cells/ $\mu\text{l}$ ; counts larger than this are considered unhealthy and serve as a diagnostic parameter for leukemia. ALL is generally discovered when the disease becomes symptomatic or

when the WBC counts are high in a blood test. By the time one of these symptoms occurs, the disease becomes challenging to treat as the leukemic cells can invade the central nervous system, testicles, or other vital organs (Pui 2006; Jabbour et al. 2010).

### 1.3 Current Treatment

Leukemia treatment aims to induce remission, defined as the absence of measurable leukemic cells. Currently, the standard treatment for ALL is chemotherapy, combining anti-leukemic medications that affect cell growth. Chemotherapy is divided into three phases: Remission induction, Intensification, and Maintenance. The Remission induction phase lasts for a month and aims to eliminate progenitor cells from the blood. The intensification phase uses increased doses of chemotherapy to reduce tumor load further and can last between one to three months. The maintenance phase lasts for at least two years at lower doses but can be interrupted by the intensification phase.

Due to risk-adapted treatments, the 5-year survival rate of newly diagnosed adults has increased from under 10% to over 90% within the last three decades (Siegel et al. 2015; Della Starza et al. 2019). However, the disease returns in more than 50% of cured adult patients after successful treatment (Gökbuget et al. 2012). Such relapsed leukemias are likely to respond unfavorably to chemotherapy and require more intense treatment. The current profile of chemotherapy drugs already causes severe toxicity that leads to infections and other complications (Schmiegelow et al. 2017), even death in 2-3% of the cases (Prucker et al. 2009; Stary et al. 2014). Leukemia can sometimes also develop resistance to chemotherapy. Patients with such unfavorable responses to chemotherapy are suggested to undergo allogeneic bone marrow transplant.

### 1.4 Recent Achievements

As a modern alternative, patients with the relapsed disease may also be staged for targeted treatments, such as immunotherapy. The adaptive immune system is capable of identifying different objects through protein receptors. A recent bi-specific antibody (protein macromolecule) construct, Blinatumomab (Nagorsen and Baeuerle 2011), showed an increase in remission rates, and longer overall survival with manageable toxic effects (Kantarjian et al. 2017). This antibody on one end binds to the killer T cells and on the other end binds to lymphoid progenitor destined to differentiate into B cells. The binding with a target induces formation of tethering knobs as the immunological synapse. This formation leads to the death of the target cell. The killer T cells also proliferate due to this effector function. The process of killer T cells killing several targets one after another is known as serial killing though T cells can run out

of ammunition and become refractory.

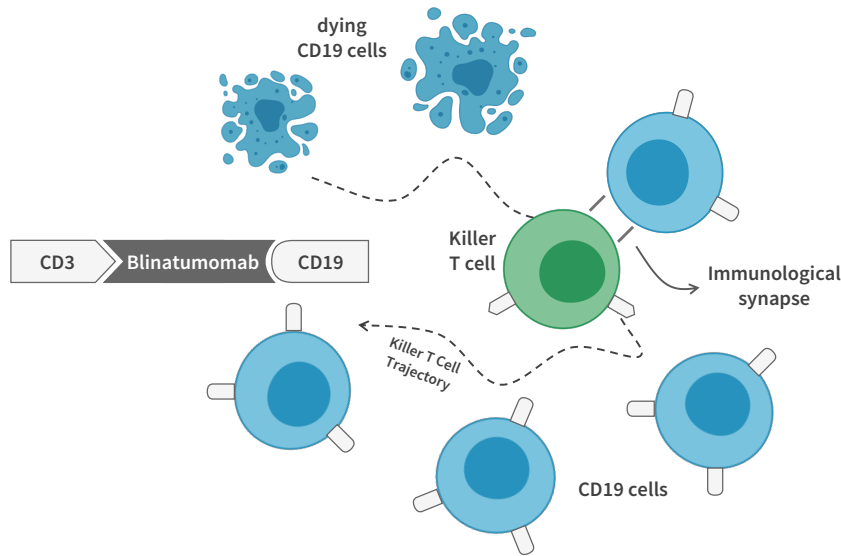


Figure 1.2: **The role of Blinatumomab in immunotherapy.** Blinatumomab is a bi-specific T cell engager antibody, that binds on one end to CD3 macromolecules, present on the surface of T cells. On other end it binds to CD19 macromolecules, present on lymphoid progenitors primed to differentiate into B cells. This binding induces the effector function of T cells and make them kill multiple lymphoid progenitor cells.

Both types of treatment rapidly decrease the leukemic cell counts below the resolution of the routine microscopy. The use of highly sensitive technologies like flow cytometry and polymerase chain reaction has allowed the detection of low levels, accurate up to 1 in  $10^6$  cells, of leukemia. An independent predictor, Minimal residual disease (MRD), has shown notable prognostic importance during recent efforts to develop personalized treatment strategies. The presence of persistent leukemic blasts after treatment at a level below the limit of conventional morphologic detection is defined as MRD positivity. This factor is associated with disease aggression, treatment response, and drug resistance (Bassan et al. 2019).

## 1.5 Literature Survey

The field of mathematical oncology is as old as the work of Knudson (1971), well-known as the two-hit hypothesis of carcinogenesis. The work of M. Kimmel and Axelrod (1990) contrasts the growth advantage of non-resistant clones with gene deamplification in the context of tumor growth and drug resistance. The number of studies has increased since the importance of a quantitative understanding of cancer biology has been recognized. Modeling efforts have targetted various aspects of the disease like cancer initiation, progression, metastasis, heterogeneity, treatment response, as well as

resistance (Altrock et al. 2015).

Chronic leukemia has been a subject of in-depth studies and modeling growth and treatment response of the disease (Michor et al. 2005; Dingli et al. 2008). These studies focus on the mutant clone dynamics during hematopoiesis, as the drivers of chronic leukemias are believed to be the mutated stem cells. Michor et al. (2005) divide hematopoiesis into four compartments; stem cells, progenitors, differentiating and terminally differentiated cells, and represent each by linear ordinary differential equations. Werner et al. (2011) take this idea further by allowing an arbitrary number of compartments with hierarchical cell organization and its relation to the origin of cancers. Komarova (2006) use the birth-death process with mutations to track the dynamics of the disease.

The tumor microenvironment and cellular interactions have a crucial contribution to disease progression. Spatial 2D lattice-based models (Ferreira et al. 2002) followed as an effort to make cancer models more realistic. Multiscale models use a hybrid approach; discrete stochastic description for cell interactions and continuous deterministic description to model environmental factors (Macklin et al. 2009). 3D continuum simulations revealed dynamic patterns of clonal heterogeneity and their implications (Waclaw et al. 2015).

With the addition of modern targeted therapies, the cancer cells can be attacked without affecting other tissues (Nagorsen and Baeuerle 2011; Kalos et al. 2011). As a result, recent efforts have turned towards the interplay between components of the immune system and tumor (G. J. Kimmel et al. 2019).

## 1.6 Scope of this study

This study is an attempt to model the treatment response and the persistent disease, unifying the deterministic and stochastic approach flexibly. We also provide a way to analyze the stochastic behavior of the persistent disease. The leukemic cell numbers cover a wide range during the treatment and relapse. The dynamics are very ‘regular’ at large population sizes, and ordinary differential equation provides an accurate picture. This deterministic idea breaks down at small population sizes where the dynamics are irregular. To model this, we need an equally flexible mathematical object that can capture both behaviors. We propose using jump processes as the deterministic motion and fluctuations arise out of the same description. The study attempts to model immunotherapy, a novel treatment type for B cell leukemia, as a first step, to understanding the interactions taking place during the treatment. The study also makes an alternative approach to understanding chemotherapy by using

two types of cells that are affected differently during chemotherapy.

The stochastic models used in the study features diffusion matrices that are not limited to linear terms, and diagonal entries to find more accurate covariance for smaller populations. We exploit the idea of random walks for stochastic analyses of minimal residual disease. All the mathematical tools required to derive the stochastic model and analyze are compiled in the methods section. There are dedicated divisions for chemotherapy and immunotherapy, that covers necessary details of the treatments and implementation of the tools.

## 1.7 Objectives

1. To understand the effect of existing treatments on the disease.
2. To investigate the contribution of residual disease in the relapse.
3. To optimize treatment strategies in ways that reduce the adverse side effects.

# Chapter 2

## Methods

### 2.1 Outline

Jump processes can provide a convenient description for any system, such as a population of different interacting objects: individuals, cells, or particles. This description is flexible in the sense that one can obtain macroscopic laws of motion and the microscopic random nature of the system. To obtain such a description, we start by writing chemical reactions representing the biological process happening in the system of interest. Chemical reactions provide quantitative change occurring in the system as well as the rate of reaction, that is how often the biological process takes place. With the combined information of all the biological processes, one can write down an equation called the master equation. This equation describes the quantitative change in the total number of each interacting cell in a probabilistic manner.

To investigate the behavior of the disease under the effect of microscopic transitions, we make use of the random walk. While studying the random walk, one is usually interested in phenomena where the object undergoing a random walk reaches a specified state of the system or the exact numbers of the cells in the population. To leverage the analysis techniques developed for a random walk, we need to convert our description into a compatible form, that is the Fokker-Planck equation. The popularity of this equation opens the door for the translation of dynamics into differential equations.

The two treatment types, chemotherapy, and immunotherapy, affect the disease in a fundamentally different way. To maintain this distinction, we model them separately. To avoid the derivation twice and reduce the effort, we first present the mathematical workflow, then simply plug in the details of respective treatments. The population of leukemic cells is the system of interest in chemotherapy. The killer T cell population

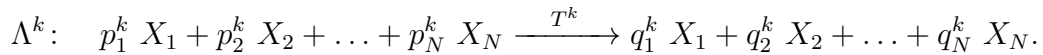
and the disease combined is the system of interest in immunotherapy.

Some common assumptions are as followed: It is assumed that the system is Markovian; that is, the future state of the disease depends only on the most recent state. It is also assumed that the system is well-mixed, such that the cells are evenly distributed in the blood. For both the treatments, the therapeutic agents, i.e., chemotherapy medication and Blinatumomab for immunotherapy, are present in a constant and non-limiting concentration.

## 2.2 Reactions

To capture the quantitative changes occurring in the system, we need to track the biological interactions. Each process takes place at a specific frequency, changing the total number of involved cell types. We use chemical reactions to capture the change in numbers and transition probabilities to capture reaction frequencies.

Consider  $N$  interacting cell types  $X_i$ ;  $i = 1, 2, \dots, N$ , undergoing  $M$  different reactions  $\Lambda^k$ ;  $k = 1, 2, \dots, M$ . Let us denote the total number of each cell type  $X_i$  as  $n_i$ . The rate associated with setting off of each reaction  $\Lambda^k$  is represented by  $T^k$ . Each reaction  $\Lambda^k$  can be written as



Where  $p_i^k$  and  $q_i^k$  are the quantities of reactant cell type  $X_i$  and product cell type  $X_i$  in reaction  $\Lambda^k$ . Then for each reaction  $\Lambda^k$  one can write the following

$$\begin{aligned} \mathbf{p}^k &= (p_1^k, p_2^k, \dots, p_N^k) \\ \mathbf{q}^k &= (q_1^k, q_2^k, \dots, q_N^k) \\ \mathbf{r}^k &= \mathbf{q}^k - \mathbf{p}^k. \end{aligned}$$

Each reaction  $\Lambda^k$  changes the count of different cell types, i.e., the state of the system changes from  $\mathbf{n}$  to  $\mathbf{n} + \mathbf{r}^k$ .

## 2.3 Master Equation

The action narrated by all the reactions and their respective rates can be described by a master equation. This equation is also known as the differential Chapman-Kolmogorov



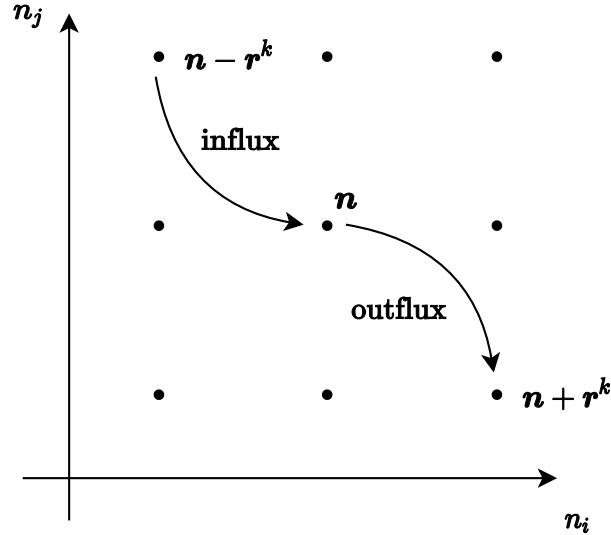


Figure 2.1: **Flux created by the reactions.** The reaction ending in the state  $\mathbf{n}$  acts as an influx for  $\Pr(\mathbf{n}, t)$  and reactions starting from the state  $\mathbf{n}$  acts as an outflux for  $\Pr(\mathbf{n}, t)$ .

equation in the literature of stochastic processes.

$$\partial_\tau \Pr(\mathbf{n}, \tau) = \sum_{\mathbf{n}' \neq \mathbf{n}} [T(\mathbf{n}') \Pr(\mathbf{n}', \tau) - T(\mathbf{n}) \Pr(\mathbf{n}, \tau)].$$

Where  $\Pr(\mathbf{n}, \tau)$  is the probability that there are  $n_i$  cells of type  $X_i$  at time  $\tau$ . The rate  $T(\mathbf{n})$  is the transition rate of the population from the focal state  $\mathbf{n}$  to a neighboring state  $\mathbf{n}'$ . The transition rate, in general, is a function of the counts of cell types involved in the reactions.

The rate of change of  $\Pr(\mathbf{n}, \tau)$  at time  $\tau$  is governed by the difference between incoming and outgoing probability flux. For our reaction system, the  $M$  reactions establish the probability flux between the states.

$$\partial_\tau \Pr(\mathbf{n}, \tau) = \underbrace{\sum_{k=1}^M T^k(\mathbf{n} - \mathbf{r}^k) \Pr(\mathbf{n} - \mathbf{r}^k, \tau)}_{\text{influx to } \mathbf{n}} - \underbrace{\Pr(\mathbf{n}, \tau) \sum_{k=1}^M T^k(\mathbf{n})}_{\text{outflux from } \mathbf{n}}. \quad (2.1)$$

## 2.4 Diffusion Approximation

Let us now scale the variables  $\mathbf{n}$  by the inverse of the system size  $R^2$  so that the number density  $\mathbf{x}$  is approximately continuous for sufficiently large system. We also scale the time  $\tau$  such that the transition rate from  $\mathbf{n}$  to  $\mathbf{n} - \mathbf{r}^k$  is same as the transition

rate from  $\mathbf{x}$  to  $\mathbf{x} - \frac{1}{R^2}\mathbf{r}^k$ .

$$\mathbf{x} = \frac{1}{R^2}\mathbf{n}; \quad t = \frac{1}{R^2}\tau.$$

The influx terms are functions of neighboring states  $\mathbf{x} - \frac{1}{R^2}\mathbf{r}^k$ , whereas the outflux terms are function of the focal state  $\mathbf{x}$ . Let us now denote  $P = \Pr(\mathbf{x}, t)$  and  $T^k = T^k(\mathbf{x})$  and consider the Taylor series around state the  $\mathbf{x}$  up to second order  $\frac{1}{R^4}$

$$\begin{aligned} \Pr(\mathbf{x} - \frac{1}{R^2}\mathbf{r}^k, t) &\approx P - \frac{1}{R^2} \sum_{i=1}^N r_i^k \partial_{x_i} P + \frac{1}{2R^4} \sum_{i=1}^N \sum_{j=1}^N r_i^k r_j^k \partial_{x_i} \partial_{x_j} P \\ T^k(\mathbf{x} - \frac{1}{R^2}\mathbf{r}^k) &\approx T^k - \frac{1}{R^2} \sum_{i=1}^N r_i^k \partial_{x_i} T^k + \frac{1}{2R^4} \sum_{i=1}^N \sum_{j=1}^N r_i^k r_j^k \partial_{x_i} \partial_{x_j} T^k \end{aligned} \quad (2.2)$$

Substitute Equation 2.2 into Equation 2.1, we find

$$\begin{aligned} \partial_t P &= \sum_{k=1}^M \left[ \left( P - \frac{1}{R^2} \sum_{i=1}^N r_i^k \partial_{x_i} P + \frac{1}{2R^4} \sum_{i=1}^N \sum_{j=1}^N r_i^k r_j^k \partial_{x_i} \partial_{x_j} P \right) \right. \\ &\quad \left. \left( T^k - \frac{1}{R^2} \sum_{i=1}^N r_i^k \partial_{x_i} T^k + \frac{1}{2R^4} \sum_{i=1}^N \sum_{j=1}^N r_i^k r_j^k \partial_{x_i} \partial_{x_j} T^k \right) - P T^k \right]. \end{aligned}$$

The zeroth order terms cancel out with the outflux terms. If we only consider the terms up to the second order  $\frac{1}{R^4}$

$$\partial_t P = \sum_{k=1}^M \left[ -\frac{1}{R^2} \sum_{i=1}^N r_i^k \partial_{x_i} [T^k P] + \frac{1}{2R^4} \sum_{i=1}^N \sum_{j=1}^N r_i^k r_j^k \partial_{x_i} \partial_{x_j} [T^k P] \right].$$

Evaluating the sum over all reactions gives us the Fokker-Planck equation.

$$\begin{aligned} \partial_t \Pr(\mathbf{x}, t) &= - \sum_{i=1}^N \partial_{x_i} [a_i(\mathbf{x}) \Pr(\mathbf{x}, t)] + \frac{1}{2} \sum_{i=1}^N \sum_{j=1}^N \partial_{x_i} \partial_{x_j} [b_{ij}(\mathbf{x}) \Pr(\mathbf{x}, t)] \\ a_i(\mathbf{x}) &= \frac{1}{R^2} \sum_{k=1}^M r_i^k T_k \\ b_{ij}(\mathbf{x}) &= \frac{1}{R^4} \sum_{k=1}^M r_i^k r_j^k T_k. \end{aligned} \quad (2.3)$$

## 2.5 The Fokker-Planck Equation

The Fokker-Planck equation is equivalent to the convection-diffusion equation and occurs in many other contexts under different names. Here, it describes the time evolution of probability density function  $\Pr(\mathbf{x}, t)$  of the number density  $\mathbf{x}$  at time  $t$ .

The RHS of the equation has two terms: deterministic drift and diffusion. Hence,  $\mathbf{a}(\mathbf{x})$  is called the drift vector and  $B(\mathbf{x})$  is called the diffusion matrix. Here, these terms account for the average dynamics and the random fluctuations of the system, respectively.

$$\begin{aligned} \partial_t \Pr(\mathbf{x}, t \mid \mathbf{x}_0, t_0) = & - \underbrace{\sum_{i=1}^N \partial_{x_i} [a_i(\mathbf{x}) \Pr(\mathbf{x}, t \mid \mathbf{x}_0, t_0)]}_{\text{deterministic drift}} \\ & + \underbrace{\frac{1}{2} \sum_{i=1}^N \sum_{j=1}^N \partial_{x_i} \partial_{x_j} [b_{ij}(\mathbf{x}) \Pr(\mathbf{x}, t \mid \mathbf{x}_0, t_0)]}_{\text{diffusion}}. \end{aligned} \quad (2.4)$$

Additional information is required for this equation to be useful in applications, for instance, initial conditions and boundary conditions. An initial condition  $\Pr(\mathbf{x}, t_0) = \delta(\mathbf{x} - \mathbf{x}_0)$  can also be encoded as  $\Pr(\mathbf{x}, t \mid \mathbf{x}_0, t_0)$ . The Fokker-Planck equation is valid for this conditional probability as well (Gardiner 2009). There are many types of boundary conditions which can be imposed based on the first principles, but we shall only work with absorbing boundaries, i.e.,  $\Pr(\mathbf{x}, t) = 0$  on the boundary.

## 2.6 Mean-field Limit

The system size  $R^2$  controls the relative contribution between the drift and the diffusion terms. Letting  $R^2 \rightarrow \infty$ , the equation takes form of the Liouville's equation. This form connects  $\Pr(\mathbf{x}, t)$  to the average time evolution of the state.

$$\begin{aligned} \partial_t \Pr(\mathbf{x}, t) &= - \sum_{i=1}^N \partial_{x_i} [a_i(\mathbf{x}) \Pr(\mathbf{x}, t)] \\ \implies \frac{d\mathbf{x}(t)}{dt} &= \mathbf{a}(\mathbf{x}). \end{aligned}$$

## 2.7 Stochastic Model

Equating the Fokker-Planck equation to the form given by Feynmann-Kac formula (Øksendal 2003), we get a system of Itô's stochastic differential equations (SDE). These SDEs can also be written in the form of Langevin equations.

$$\dot{\mathbf{x}} = \mathbf{a}(\mathbf{x}) + \sqrt{B}(\mathbf{x}) \boldsymbol{\xi}(t). \quad (2.5)$$

The dot over a symbol represents the derivative with respect to time  $t$ . Here,  $\mathbf{a}(\mathbf{x})$  is deterministic drift vector and  $B(\mathbf{x})$  is the diffusion matrix. The notation  $\sqrt{B}$  denotes

square root of a matrix. Any matrix  $A$  is a square root of matrix  $B$  if the matrix product  $AA$  is equal to  $B$  (Denman 1981; Björck and Hammarling 1983).

Stochastic differential equations can only rarely be solved analytically. In such cases, one resorts to numerical solutions; however, finding the square root of matrices is challenging for higher dimensions. One can write another system of stochastic differential equations with matrix  $C$  instead of  $\sqrt{B}$  such that  $CC^T = B$ . Since both follow the same Fokker-Planck equation, they are equivalent (Section 5.1, Allen 2007).

For a system with  $N$  entities and  $M \geq N$  reactions, where each reaction  $\Lambda^k$  alters the state  $\mathbf{x}$  by the amount  $\frac{1}{R^2}\mathbf{r}^k$  with transition rate  $T^k$ . One can write  $C$  such that

$$c_{ik} = r_i^k (T^k)^{\frac{1}{2}}.$$

$$\dot{\mathbf{x}} = \mathbf{a}(\mathbf{x}) + C(\mathbf{x}) \boldsymbol{\xi}^*(t). \quad (2.6)$$

Where  $\boldsymbol{\xi} = (\xi_1, \xi_2, \dots, \xi_N)$  and  $\boldsymbol{\xi}' = (\xi_1, \xi_2, \dots, \xi_M)$  and  $\xi_i$  are gaussian white noise terms such that

$$\langle \xi_i(t) \rangle = 0,$$

$$\langle \xi_i(t) \xi_j(t') \rangle = \delta(t - t').$$

## 2.8 First-passage Analysis

When the disease reaches a state of zero tumor cells, it goes extinct and cannot reappear, this is said to be an absorbing state of the system. A system based on its description can have multiple absorbing states, resulting in specific consequences, e.g. extinction. The study of meeting these conditions for the first time is known as the survival or the first-passage analysis. While Equation 2.4, called the forward equation, describes dynamics in the future the backward Fokker-Planck equation describes dynamics in the past. The forward equation is useful for prediction, i.e. inferring observed quantities in future, whereas the backward equation is more useful for studying the first passage properties.

Let us denote the forward variables as  $(\mathbf{x}', t')$  the backward variables as  $(\mathbf{x}, t)$  for first-passage analysis. Just like how the forward equation requires initial conditions and boundary conditions, the backward equation requires final conditions and boundary

conditions.

$$\begin{aligned} \partial_t \Pr(\mathbf{x}', t' | \mathbf{x}, t) &= - \sum_{i=1}^N a_i(\mathbf{x}) \partial_{x_i} \Pr(\mathbf{x}', t' | \mathbf{x}, t) \\ &\quad - \frac{1}{2} \sum_{i=1}^N \sum_{j=1}^N b_{ij}(\mathbf{x}) \partial_{x_i} \partial_{x_j} \Pr(\mathbf{x}', t' | \mathbf{x}, t). \end{aligned}$$

If the process does not explicitly depend on time, i.e.  $\mathbf{a}$  and  $B$  are function of only  $\mathbf{x}$  and not  $t$ , then it is said to be homogeneous in time. For homogeneous processes

$$\Pr(\mathbf{x}', t | \mathbf{x}, 0) = \Pr(\mathbf{x}', 0 | \mathbf{x}, -t).$$

Then the backward Fokker-Planck equation for homogeneous processes

$$\begin{aligned} \partial_t \Pr(\mathbf{x}', t | \mathbf{x}, 0) &= \sum_{i=1}^N a_i(\mathbf{x}) \partial_{x_i} \Pr(\mathbf{x}', t | \mathbf{x}, 0) \\ &\quad + \frac{1}{2} \sum_{i=1}^N \sum_{j=1}^N b_{ij}(\mathbf{x}) \partial_{x_i} \partial_{x_j} \Pr(\mathbf{x}', t | \mathbf{x}, 0). \end{aligned} \tag{2.7}$$

## 2.9 Probability of First-exit

We now make an analogy between a particle experiencing random fluctuation in a region  $\mathcal{R}$  and the state of the system. If we enumerate through different instances of this motion with a fixed initial condition, i.e. a starting point of the particle, we find that it hits different point on the boundary  $\mathcal{S}$  with different probability. We are interested in this probability of particle exiting as a function of the initial condition. Turning this problem around we ask for the probability of reaching a point, in past, in the region  $\mathcal{R}$  starting from a fixed final condition.

The probability to exit from a region  $\mathcal{R}$  through an infinitesimal surface element  $d\mathcal{S}(\mathbf{z})$  at a point  $\mathbf{z}$  on the surface  $\mathcal{S}$  for the first time given that you start at a point  $\mathbf{x}$  is said to be the first-exit probability. The probability that particle exits through  $d\mathcal{S}(\mathbf{z})$  after time  $t$  can be obtained by collecting the flux exited through  $d\mathcal{S}(\mathbf{z})$  after time  $t$

$$g(\mathbf{z}, \mathbf{x}, t) |d\mathcal{S}(\mathbf{z})| = \int_t^\infty dt' \mathbf{J}(\mathbf{z}, t' | \mathbf{x}, 0) \cdot d\mathcal{S}(\mathbf{z}). \tag{2.8}$$

where components of the flux  $\mathbf{J}(\mathbf{z}, t' | \mathbf{x}, 0)$  are defined as

$$J_i(\mathbf{z}, t' | \mathbf{x}, 0) = a_i(\mathbf{z}) \Pr(\mathbf{z}, t' | \mathbf{x}, 0) - \frac{1}{2} \sum_{j=1}^N \partial_{x_j} b_{ij}(\mathbf{z}) \Pr(\mathbf{z}, t' | \mathbf{x}, 0).$$

such that the forward Fokker-Planck equation takes the form of well-known continuity equation.

$$\partial_t \Pr(\mathbf{x}, t) + \sum_{i=1}^N \partial_{x_i} J_i(\mathbf{x}, t) = 0.$$

Using the definition of  $g(\mathbf{z}, \mathbf{x}, t)$  (Equation 2.8) and the fact that  $\mathbf{J}(\mathbf{z}, t' | \mathbf{x}, 0)$  also follows the backward Fokker-Planck equation (Equation 2.7) we get the following equation (Section 5.5.4, Gardiner 2009).

$$\partial_t g(\mathbf{z}, \mathbf{x}, t) = \sum_{i=1}^N a_i(\mathbf{x}) \partial_{x_i} g(\mathbf{z}, \mathbf{x}, t) + \frac{1}{2} \sum_{i=1}^N \sum_{j=1}^N b_{ij}(\mathbf{x}) \partial_{x_i} \partial_{x_j} g(\mathbf{z}, \mathbf{x}, t). \quad (2.9)$$

Now let us denote the probability of ultimate exit  $g(\mathbf{z}, \mathbf{x}, 0)$  as  $\pi_{\mathbf{z}}(\mathbf{x})$ . Note that for any deterministic initial condition  $\Pr(\mathbf{z}, 0 | \mathbf{x}, 0) = \delta(\mathbf{z} - \mathbf{x})$  the probability density is concentrated at the point  $\mathbf{x}$  at time  $t = 0$ . Thus, the flux also only exists in an infinitesimal neighborhood of  $\mathbf{x}$ . Therefore  $J(\mathbf{z}, 0 | \mathbf{x}, 0)$  must vanish for every point  $\mathbf{x} \neq \mathbf{z}$  at time  $t = 0$ . Hence, by letting  $t \rightarrow 0$  the right hand side of the equation vanishes as it is the integration of  $\mathbf{J}(\mathbf{z}, t' | \mathbf{x}, 0)$ .

$$0 = \sum_{i=1}^N a_i(\mathbf{x}) \partial_{x_i} \pi_{\mathbf{z}}(\mathbf{x}) + \frac{1}{2} \sum_{i=1}^N \sum_{j=1}^N b_{ij}(\mathbf{x}) \partial_{x_i} \partial_{x_j} \pi_{\mathbf{z}}(\mathbf{x}).$$

Suppose that particles can only exit through  $d\mathcal{S}(\mathbf{z})$  then boundary conditions for the backward Fokker-Planck equation of  $\pi_{\mathbf{z}}(\mathbf{x})$  is

$$\pi_{\mathbf{z}}(\mathbf{x}) = \delta_{\mathcal{S}}(\mathbf{z} - \mathbf{x}).$$

## 2.10 Mean First-exit Time

We also want to know how long does a particle take to exit a region  $\mathcal{R}$  for the first time. This can similarly be rephrased as time taken to reach a point in region  $\mathcal{R}$  given a final condition. Let the particle initially be at  $\mathbf{x}$ , the probability it is somewhere within  $\mathcal{R}$  at time  $t$  is

$$G(\mathbf{x}, t) = \int_{\mathcal{R}} d\mathbf{x}' \Pr(\mathbf{x}', t | \mathbf{x}, 0). \quad (2.10)$$

Let us denote the time particle leaves the region  $\mathcal{R}$  for first time as  $T$ . For any time  $t$ ,  $T \geq t$  means that particle has not left the region  $\mathcal{R}$ . Thus,  $\Pr(T \geq t)$  is the probability it is still in the region  $\mathcal{R}$  at time  $t$

$$\Pr(T \geq t) = G(\mathbf{x}, t). \quad (2.11)$$

Integrating the backward Fokker-Planck equation (Equation 2.7) with respect to  $d\mathbf{x}'$  and using the definition of  $G(\mathbf{x}, t)$  (Equation 2.10) we find that  $G(\mathbf{x}, t)$  also satisfies the backward equation.

$$\partial_t G(\mathbf{x}, t) = \sum_{i=1}^N a_i(\mathbf{x}) \partial_{x_i} G(\mathbf{x}, t) + \frac{1}{2} \sum_{i=1}^N \sum_{j=1}^N b_{ij}(\mathbf{x}) \partial_{x_i} \partial_{x_j} G(\mathbf{x}, t). \quad (2.12)$$

With the initial conditions  $\Pr(\mathbf{x}', 0 \mid \mathbf{x}, 0) = \delta(\mathbf{x}' - \mathbf{x})$  the  $G(\mathbf{x}, t)$  takes the following values

$$G(\mathbf{x}, t) = \begin{cases} 1 & \mathbf{x} \in \mathcal{R} \\ 0 & \text{elsewhere} \end{cases}$$

We impose absorbing boundary condition for  $G(\mathbf{x}, t)$  as particles starting anywhere on the boundary  $\mathcal{S}$  will exit immediately  $T = 0$ . Thus when  $\mathbf{x}$  is on the boundary,  $\Pr(T \geq t) = 0$  and

$$G(\mathbf{x}, t) = 0, \quad \mathbf{x} \in \mathcal{S}.$$

Since  $G(\mathbf{x}, t)$  is the complementary cumulative distribution function of  $T$ , because of the form of Equation 2.11, the mean of any function  $f(T)$  is

$$\langle f(T) \rangle = - \int_0^{\infty} f(t) dG(\mathbf{x}, t).$$

and thus, the mean exit time  $T(\mathbf{x}) = \langle T \rangle$  is given by

$$\begin{aligned} T(x) &= - \int_0^{\infty} t \partial_t G(\mathbf{x}, t) dt \\ &= \int_0^{\infty} G(\mathbf{x}, t) dt. \end{aligned} \quad (2.13)$$

Substituting this in Equation 2.12 we get

$$-1 = \sum_{i=1}^N a_i(\mathbf{x}) \partial_{x_i} T(\mathbf{x}) + \frac{1}{2} \sum_{i=1}^N \sum_{j=1}^N b_{ij}(\mathbf{x}) \partial_{x_i} \partial_{x_j} T(\mathbf{x}). \quad (2.14)$$

with absorbing boundary conditions

$$T(\mathbf{x}) = 0, \quad \mathbf{x} \in \mathcal{S}.$$

## 2.11 Numerical Solutions

We used Gillespie's stochastic simulation algorithm (Gillespie 1977) to simulate the system of reactions. This algorithm is reliable and used widely in the field to produce an exact instance of the master equation. The major drawback of this algorithm is high computational complexity arising from the need to simulate each reaction firing separately. Due to this way of simulations, the computation time scales with the number of interacting cells.

The Fokker-Planck equation can be solved using standard finite difference methods for parabolic partial differential equations. The alternating direction implicit method was preferred over the Crank-Nicholson method and the explicit forward-time-central-space method. The reason being the alternate-direction implicit method offers the best timestep to resolution ratio. However, the Fokker-Planck equation is stiff for the majority of the parameter space and gives rise to a trade-off between resolution and computation time. Taking into account that cells follow exponential growths needing large 2D domains contribute to the difficulty.

To escape from both; simulation of the master equation and numerically solving the Fokker-Planck equation, a more robust strategy was called for. Solving Ito's stochastic differential equations is identical to solving the afore-mentioned equations yet numerically less resource hungry. These can be solved with the Euler-Maruyama method (Kloeden and Platen 1992), which is a generalization of Euler's method for ordinary differential equations. However, in recent years there has been development in stochastic Runge-Kutta (SRK) methods. These methods offer higher efficiency with a considerable reduction in computational complexity (Rößler 2009). A python package 'sdeint', that features an implementation of stochastic Runge-Kutta, was used to numerically solve stochastic differential equations (Aburn 2015).



# Chapter 3

## Model for Chemotherapy

Symbol	Description	Default values
$X$	slowly proliferating cells	
$Y$	rapidly proliferating cells	
$r_X, r_Y$	proliferation rate constants	0.2, 1 $day^{-1}$
$p_X, p_Y$	switching rate constants	0.02, 0.02
$\alpha$	strength of chemotherapy	2

Table 3.1: **Symbols used for variables and parameters in the chemotherapy model.**

Chemotherapy targets leukemic cells differently, proportional to their growth rate, i.e., the faster-growing cells experience more mortality rates. To understand the role played by the slowly growing leukemic cells in relapse, we assume two types of leukemic cells: slowly proliferating and rapidly proliferating cells. It is assumed that the slow and fast-growing subpopulations can switch their types, i.e., slowly growing cells can change into the rapidly growing cell and vice-versa. The slowly proliferating cells are denoted as  $X$  and rapidly proliferating cells as  $Y$ .

Reactions corresponding to the biological processes carried out by cells are summarized in Table 3.2. The per-capita cell growth rates are denoted as  $r_X, r_Y$ , and cell proliferation is depicted by reactions 3.1 and 3.2. The per-capita cell-type switching rates are denoted  $p_X, p_Y$ , and the conversion between the tumor cell types is captured by reactions 3.3 and 3.4. The reactions 3.5 and 3.6 that symbolize the death of tumor cells where  $\alpha$  is the strength of chemotherapy. The  $\alpha$  is the proportionality constant for the death of leukemic cells.

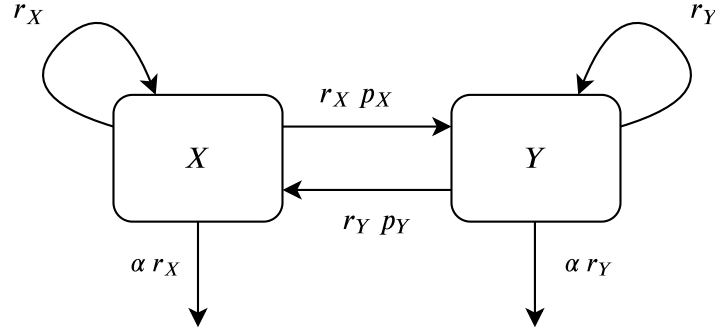


Figure 3.1: **Illustration of the chemotherapy model.** The slow and fast cell types, denoted  $X$  and  $Y$ , proliferate with respective growth rates  $r_X, r_Y$ . Both the cell types switch to the other type with rates  $r_X p_X, r_Y p_Y$ , respectively. During the chemotherapy there is an additional mortality rate that is proportional to the growth rate of the cell types. The proportionality constant, i.e., the strength of the chemotherapy is  $\alpha$ .

Reaction	Rate	Change vector	
$X \longrightarrow X + X$	$r_X X$	$\mathbf{r}^1 = (1, 0)$	(3.1)
$Y \longrightarrow Y + Y$	$r_Y Y$	$\mathbf{r}^2 = (0, 1)$	(3.2)
$X \longrightarrow Y$	$r_X p_X X$	$\mathbf{r}^3 = (-1, 1)$	(3.3)
$Y \longrightarrow X$	$r_Y p_Y Y$	$\mathbf{r}^4 = (1, -1)$	(3.4)
$X \longrightarrow \phi$	$\alpha r_X X$	$\mathbf{r}^5 = (-1, 0)$	(3.5)
$Y \longrightarrow \phi$	$\alpha r_Y Y$	$\mathbf{r}^6 = (0, -1)$	(3.6)

Table 3.2: **Reactions used in the chemotherapy model.**

### 3.1 Master Equation

Substituting the reaction rates and change vectors in Equation 2.1 we get the following master equation for chemotherapy

$$\begin{aligned}
 \therefore \partial_t \Pr(n_X, n_Y, t) = & r_X (n_X - 1) \Pr(n_X - 1, n_Y, t) + r_Y (n_Y - 1) \Pr(n_X, n_Y - 1, t) \\
 & + r_X p_X (n_X + 1) \Pr(n_X + 1, n_Y - 1, t) + r_Y p_Y (n_Y + 1) \Pr(n_X - 1, n_Y + 1, t) \\
 & + \alpha r_X (n_X + 1) \Pr(n_X + 1, n_Y, t) + \alpha r_Y (n_Y + 1) \Pr(n_X, n_Y + 1, t) \\
 & - [r_X (1 + p_X + \alpha) n_X + r_Y (1 + p_Y + \alpha) n_Y] \Pr(n_X, n_Y, t)
 \end{aligned} \tag{3.7}$$

## 3.2 Fokker-Planck Equation

Carrying out Taylor series expansion of the master equation as directed in section 2.4 we obtain the deterministic drift vector  $\mathbf{a}^c$ , the diffusion matrix  $B^c$  and the alternative diffusion matrix  $C^c$  obtained from the chemotherapy reaction rates (Table 3.2).

$$\begin{aligned}
 \mathbf{a}^c(\mathbf{x}) &= \begin{bmatrix} r_X (1 - p_X - \alpha) x + r_Y p_Y y \\ r_Y (1 - p_Y - \alpha) y + r_X p_X x \end{bmatrix} \\
 B^c(\mathbf{x}) &= \begin{bmatrix} r_X (1 + p_X + \alpha) x + r_Y p_Y y & -(r_X p_X x + r_Y p_Y y) \\ -(r_X p_X x + r_Y p_Y y) & r_Y (1 + p_Y + \alpha) y + r_X p_X x \end{bmatrix} \\
 C^c(\mathbf{x}) &= \begin{bmatrix} \sqrt{r_X x} & -\sqrt{r_X p_X x} & \sqrt{r_Y p_Y y} & -\sqrt{\alpha r_X x} \\ & \sqrt{r_Y y} & \sqrt{r_X p_X x} & -\sqrt{r_Y p_Y y} \\ & & & -\sqrt{\alpha r_Y y} \end{bmatrix} \tag{3.8}
 \end{aligned}$$

Substituting the drift vector and diffusion matrices in the Fokker-Planck equation (Equation 2.4) we get the Fokker-Planck equation for chemotherapy.

$$\partial_t \Pr(\mathbf{x}, t) = - \sum_{i=1}^2 \partial_{x_i} [a_i^c(\mathbf{x}) \Pr(\mathbf{x}, t)] + \sum_{i=1}^2 \sum_{j=1}^2 \partial_{x_i} \partial_{x_j} [b_{ij}^c(\mathbf{x}) \Pr(\mathbf{x}, t)]$$

## 3.3 Mean-field Limit

Application of Liouville's theorem leads to a system of ordinary differential equations.

$$\dot{\mathbf{x}} = \mathbf{a}^c(\mathbf{x})$$

The mean-field model is linear and has one fixed point at  $(0, 0)$ .

$$\mathbf{x}_{tr} = (0, 0)$$

Linearizing around the fixed point we get the following Jacobian matrix

$$\mathbf{J}(\mathbf{x}_{tr}) = \begin{bmatrix} r_X (1 - p_X - \alpha) & r_Y p_Y \\ r_X p_X & r_Y (1 - p_Y - \alpha) \end{bmatrix}$$

Let us consider the following 2x2 matrix

$$\begin{bmatrix} a & b \\ d & c \end{bmatrix}.$$

Where

$$\begin{aligned} a &= r_X (1 - p_X - \alpha) \\ b &= r_Y p_Y \\ c &= r_Y (1 - p_Y - \alpha) \\ d &= r_X p_X. \end{aligned}$$

The eigenvalues of the Jacobian matrix  $\mathbf{J}(\mathbf{x}_{tr})$  are

$$\lambda_{\pm} = \frac{1}{2} \left[ a + c \pm \sqrt{(a - c)^2 + 4bd} \right].$$

Now, the cell type switching rates  $b, d$  are always positive (Table 3.1). The realized growth rates  $a, c$  are negative during chemotherapy as  $\alpha = 2$ ; and are positive otherwise because  $\alpha = 0$ . The term  $(a - c)^2$  is always positive, that means  $(a - c)^2 + 4bd$  is positive, hence eigenvalues are real.

For very small switching rates  $b, d \ll 1$  (Table 3.1), we can ignore  $4bd$  and  $\lambda_{\pm} \approx \frac{1}{2} [a + c \pm |a - c|]$ . In case of chemotherapy  $0 > a > c$ , and otherwise  $0 < a < c$ . Thus for chemotherapy,  $\lambda_+ \approx a$ ;  $\lambda_- \approx c$  and otherwise  $\lambda_+ \approx c$ ;  $\lambda_- \approx a$ .

In chemotherapy,  $\mathbf{x}_{tr}$  is a stable fixed point as the eigenvalues are negative. Otherwise, it is an unstable fixed point because eigenvalues are positive. The largest eigenvalue drives the system and for low switching rates, the growth rate of corresponding subpopulation determines the growth rate of the disease.

To dissect the effect of cell type switching, we simulate four different cases (Figure 3.2). The extinction of a cell type is defined as the absence of the cell type, i.e.,  $x_i = 0$ .

### Case 1 : No cell type switching

No switching of cell types was allowed in this case, i.e.  $p_X = p_Y = 0$ . In this case, the populations did not survive until the end of the treatment and went extinct.

### Case 2 : only slow to fast cell type switching

Only slowly growing cells were allowed to switch into rapidly growing cells, that is  $p_X = 0.02$ ,  $p_Y = 0$ . Both the populations faced extinction in this case.

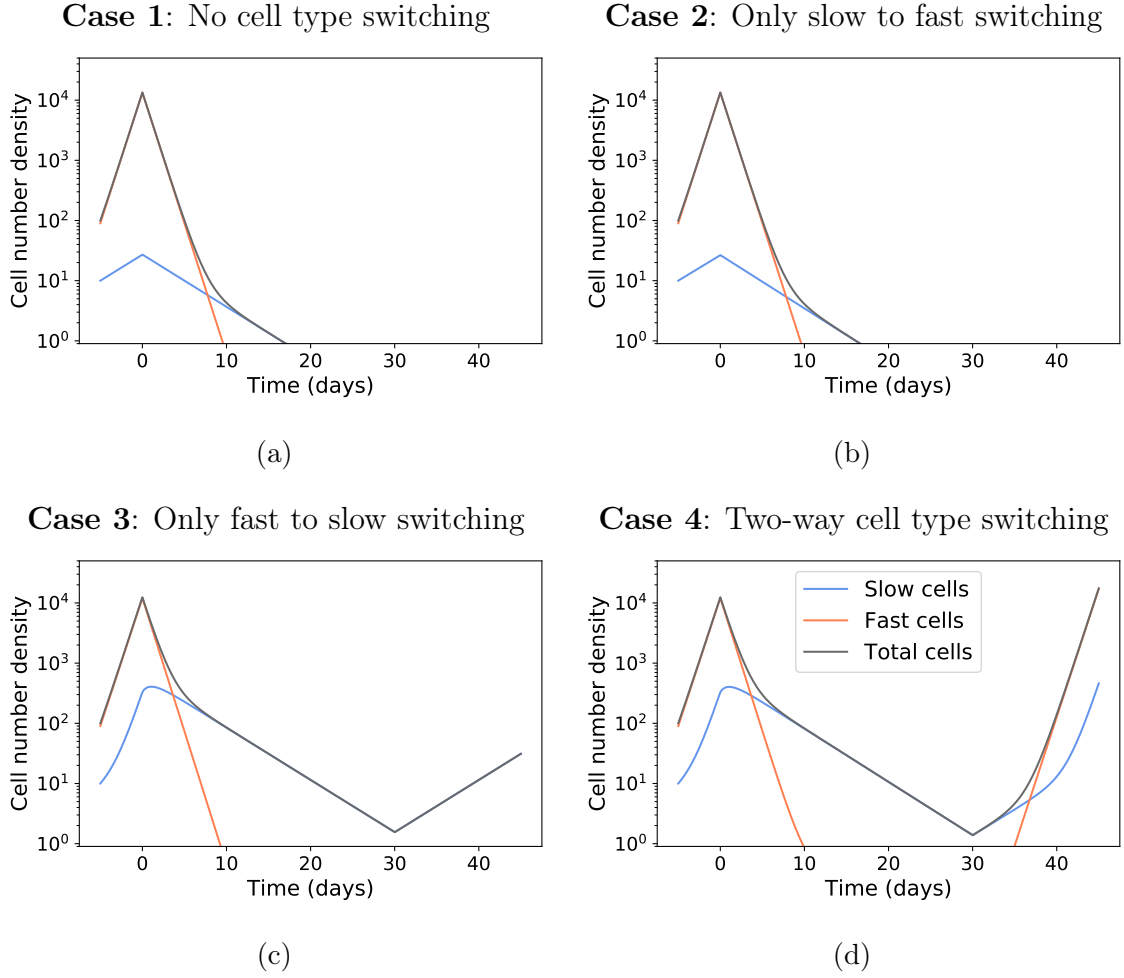


Figure 3.2: **Mean-field dynamics of slow and fast cells under chemotherapy.** The treatment starts on day 0 and lasts for 30 days. The blue and orange lines represent the slow and fast cell types, respectively. The gray line represents the total number of leukemic cells. The initial condition was  $\mathbf{x} = (10, 90)$  for all cases. The growth rate of slow cells  $r_X = 0.2$ , the growth rate of fast cells  $r_Y = 1$ , growth rate of slow cells  $r_X = 0.2$ , strength of chemotherapy  $\alpha = 2$ . Panel (a) no switching rate,  $p_X = p_Y = 0$  result in extinction of both cell type with absence of a relapse. Panel (b) only slow to fast switching rate  $p_X = 0.02$ , results in extinction of both the cell types. Panel (c) fast to slow switching rate  $p_Y = 0.02$ , results in extinction of fast cell with a slow relapse. Panel (d) two-way switching rate  $p_X = p_Y = 0.02$ , result in extinction of fast cells with fast relapse.

### Case 3 : only fast to slow cell type switching

Only rapidly growing cells were allowed to switch to slowly growing cells, that is  $p_X = 0$ ,  $p_Y = 0.02$ . The rapidly growing population went extinct, whereas the slowly growing population survived the treatment. The relapse following the treatment was represented by the remaining slow-growing cells.

### Case 4 : two-way cell type switching

Both the cell types are allowed to switch into each other, that is  $p_X = p_Y = 0.02$ . The slowly growing population survived the treatment while rapidly growing population faced extinction. The relapse after the treatment had both types of the cell because of the two-way switching.

At the beginning of the treatment, the slow populations did not decline right away. The influx from rapidly growing cells supported the slowly-growing populations. The support persisted until the rapidly growing cells declined below a particular value. After a specific duration into the treatment, the decline of rapidly growing cells was supported by the slowly proliferating cells. Right after the treatment, the relapse was slow, but later it was represented by the fast-growing cells.

### 3.4 Stochastic Model

Using the Feynmann-Kac formula (section 2.7), we can obtain the stochastic differential equations for chemotherapy.

$$\dot{\mathbf{x}} = \mathbf{a}^c(\mathbf{x}) + \sqrt{B^c(\mathbf{x})} \boldsymbol{\xi}(t).$$

Using the procedure to obtain the alternative system as directed in section 2.7 we get

$$\dot{\mathbf{x}} = \mathbf{a}^c(\mathbf{x}) + C^c(\mathbf{x}) \boldsymbol{\xi}^*(t).$$

### 3.5 First-passage Analysis

The exit probability through a particular exit always decay as you go away from it; i.e., there is no periodic behavior or increase in the probability. This observation is due to the boundary condition (section 2.9) and the diffusive nature of Equation 2.7. Solving this equation numerically for the entire domain, i.e. square boundary of  $\infty$  length is impossible. Thus, we solve for more feasible boundaries. The maximum chance of exit increases for larger domains; for the smaller domain (Figure 3.3a), there was a maximum 2.5% chance of exit. Whereas for a larger domain, (Figure 3.3b), there was, maximum 6% chance of exit. The system behaves according to the the original domain, therefore exit probability obtained by solving any finite boundary length will underestimate the chance of exit.

Reduction in the leukemic cell counts led to more frequent extinction. This was concluded using the first-exit probabilities (section 2.9) for the chemotherapy model. The probability of exit at  $(0, 0)$  was spread along the y-axis, i.e., the number density of

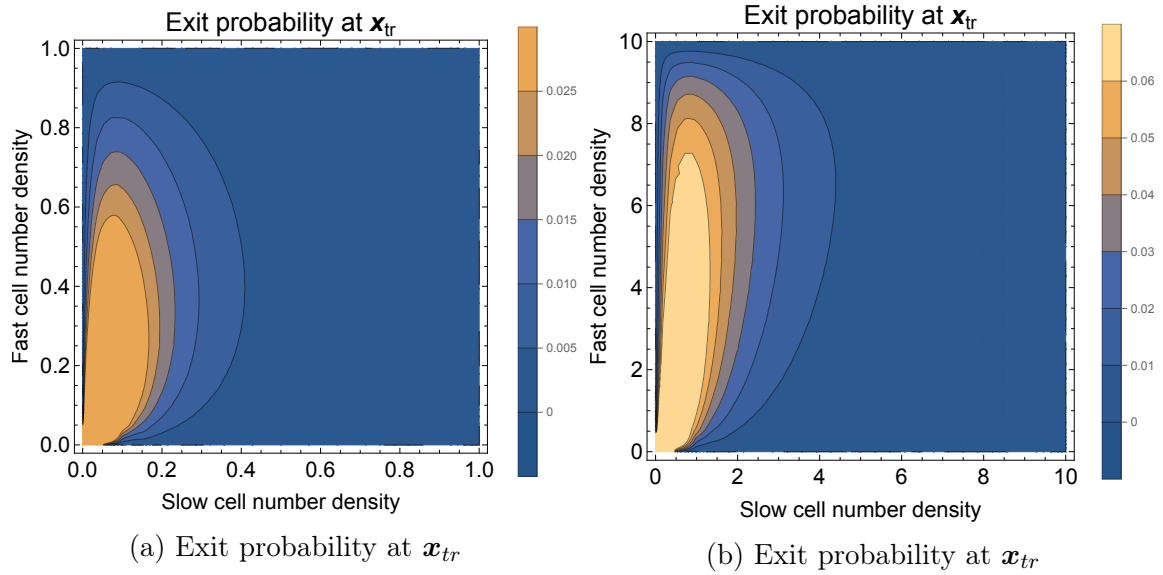


Figure 3.3: **Comparison of different boundary lengths for extinction in chemotherapy.** All the panels have equal parameter values  $r_X = 0.2$ ,  $r_Y = 1$ ,  $p_X = p_Y = 0.02$ ,  $\alpha = 2$ ,  $R = 1$ . Panel (a) shows exit probabilities at  $\mathbf{x}_{ts}$  for square boundaries of length 1 unit. Panel (b) shows exit probabilities at  $\mathbf{x}_{ts}$  for square boundaries of length 10 units. An increase of spread in exit-probabilities is observed from panel (a) to (b) as boundaries expand.

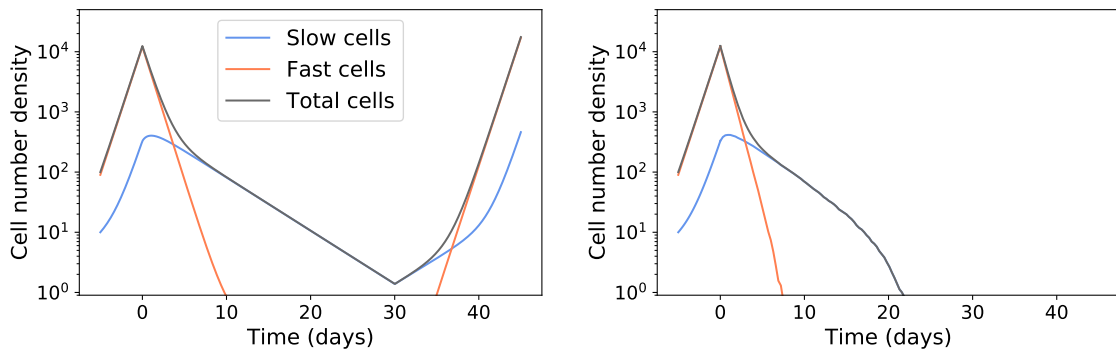


Figure 3.4: **Comparison of deterministic and stochastic trajectories of slow and fast cells under chemotherapy.** All the panels have equal parameter values  $r_X = 0.2$ ,  $r_Y = 1$ ,  $p_X = p_Y = 0.02$ ,  $\alpha = 2$ ,  $R = 1$ . Panel (a) shows deterministic trajectories for chemotherapy. Panel (b) shows stochastic trajectories for chemotherapy. Panel (b) is the average of 50 individual stochastic trajectories. The stochastic model for same parameter values predict an extinction of the disease during chemotherapy while deterministic model predicts a relapse.

fast cells. The random fluctuations realized in the population allowed it to go extinct (Figure 3.4b) even when there is no extinction in the mean-field model (Figure 3.4a).





# Chapter 4

## Model for Immunotherapy

Symbol	Description	
$X$	leukemia cells	
$Y$	cytotoxic T cells	
$r_X, r_Y$	birth rate constants	$1, 1 \text{ day}^{-1}$
$K$	T cell carrying capacity	1
$\chi$	inverse of T cell killing capacity	1
$\delta$	T cell mediated killing rate constant	$1 \text{ day}^{-1}$
$\beta$	T cell activation rate constant	$1 \text{ day}^{-1}$

Table 4.1: **Symbols used for variables and parameters in the immunotherapy model.**

Immunotherapy uses the patient's own killer T cells against the tumor. The bi-specific antibody, Blinatumomab, can bind to both killer T cells and the lymphoid progenitor cells. The binding caused by the antibody induces an immunological synapse between the killer T cells and the target cells. Formation of a synapse lead the killer T cells to release lethal molecules, making them kill the tumor cells. Moreover, this effector function of killer T cells also induces their proliferation, known as T cell activation. To understand the role played by the effector cells of the immune system, we assume two cell types: target (tumor) cells and T cells. The tumor cells are denoted as  $X$ , and the T cells are denoted as  $Y$ . The killing imposed by T cell depletes their resources and makes them refractory. The refractory T cells do not contribute to the treatment and are considered dead for the scope of this study.

Reactions corresponding to the biological interactions experienced by tumor cells and T cells are summarized in Table 4.2. The per-capita proliferation rate of tumor cells is

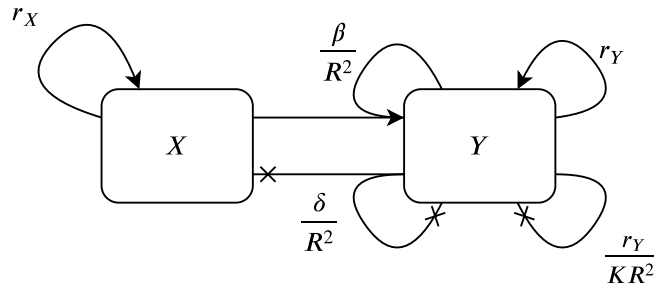


Figure 4.1: **Illustration of the immunotherapy model.** The tumor and killer T cells, denoted  $X$  and  $Y$ , proliferate with respective growth rates  $r_X, r_Y$ . The T cells are under immune regulation, with a competitive exclusion rate of  $r_Y/K$ , imposing a carrying capacity  $K$ . The presence of Blinatumomab bound target cells leads to T cell activation with the rate  $\beta$ . The T cell mediated killing takes place at the rate  $\delta$  and removes  $\chi$  T cells for target cell killed.

denoted  $r_X$ , and the tumor growth is depicted by reaction 4.1. The per-capita growth rate of T cell is denoted  $r_Y$ , and the T cell growth is represented by reaction 4.2. The immune regulation of T cells is captured by reaction 4.3 where  $K$  is the immune carrying capacity, and  $R^2$  is the total volume of blood. The activation of T cells is symbolized by reaction 4.4,  $\beta$  is the per-capita activation rate of T cells. The effector function of T cells is shown in reaction 4.5 where  $\delta$  is the per-capita killing rate, and  $\chi$  is the inverse of the average number of B cells killed by a T cell.

Reaction	Rate	Change vector
$X \longrightarrow X + X$	$r_X X$	$\mathbf{r}^1 = (1, 0)$ (4.1)
$Y \longrightarrow Y + Y$	$r_Y Y$	$\mathbf{r}^2 = (0, 1)$ (4.2)
$Y + Y \longrightarrow Y$	$\frac{r_Y}{K R^2} Y^2$	$\mathbf{r}^4 = (0, -1)$ (4.3)
$X + Y \longrightarrow X + Y + Y$	$\frac{\beta}{R^2} X Y$	$\mathbf{r}^5 = (0, 1)$ (4.4)
$X + \chi Y \longrightarrow \phi$	$\frac{\delta}{R^2} X Y$	$\mathbf{r}^3 = (-1, -\chi)$ (4.5)

Table 4.2: **Reactions used in the immunotherapy model.**

## 4.1 Master Equation

Substituting the reaction rates and change vectors in Equation 2.1 we get the following master equation for immunotherapy

$$\begin{aligned}
\therefore \partial_t \Pr(n_X, n_Y, t) &= r_X (n_X - 1) \Pr(n_X - 1, n_Y, t) \\
&+ r_Y (n_Y - 1) \Pr(n_X, n_Y - 1, t) \\
&+ \frac{r_Y}{K R^2} (n_Y + 1)^2 \Pr(n_X, n_Y + 1, t) \\
&+ \frac{\beta}{R^2} n_X (n_Y - 1) \Pr(n_X, n_Y - 1, t) \\
&+ \frac{\delta}{R^2} (n_X + 1) (n_Y + \chi) \Pr(n_X + 1, n_Y + \chi, t) \\
&- \left[ r_X n_X + \frac{\delta}{R^2} n_X n_Y \right. \\
&\left. + r_Y n_Y + \frac{r_X}{K R^2} n_Y^2 + \frac{\beta}{R^2} n_X n_Y \right] \Pr(n_X, n_Y, t)
\end{aligned} \tag{4.6}$$

## 4.2 Fokker-Planck Equation

The deterministic drift vector  $\mathbf{a}^{\mathcal{I}}$ , the diffusion matrix  $B^{\mathcal{I}}$  and the alternative diffusion matrix  $C^{\mathcal{I}}$  are obtained by performing Taylor series expansion of the master equation as directed in section 2.4 using the immunotherapy reaction rates (Table 4.2).

$$\begin{aligned}
\mathbf{a}^{\mathcal{I}}(\mathbf{x}) &= \begin{bmatrix} r_X x - \delta x y \\ r_Y y (1 - \frac{y}{K}) + (\beta - \delta \chi) x y \end{bmatrix} \\
B^{\mathcal{I}}(\mathbf{x}) &= \begin{bmatrix} r_X x + \delta x y & \chi \delta x y \\ \chi \delta x y & r_Y y (1 + \frac{y}{K}) + (\beta + \chi^2 \delta) x y \end{bmatrix} \\
C^{\mathcal{I}}(\mathbf{x}) &= \begin{bmatrix} \sqrt{r_X x} & & & -\sqrt{\delta x y} \\ & \sqrt{r_Y y} & -\sqrt{\frac{r_Y}{K} y^2} & \sqrt{\beta x y} & -\chi \sqrt{\delta x y} \end{bmatrix}
\end{aligned} \tag{4.7}$$

Substituting the drift vector and diffusion matrices in the Fokker-Planck equation (Equation 2.4) we get the Fokker-Planck equation for immunotherapy.

$$\partial_t \Pr(\mathbf{x}, t) = - \sum_{i=1}^2 \partial_{x_i} [a_i^{\mathcal{I}}(\mathbf{x}) \Pr(\mathbf{x}, t)] + \sum_{i=1}^2 \sum_{j=1}^2 \partial_{x_i} \partial_{x_j} [b_{ij}^{\mathcal{I}}(\mathbf{x}) \Pr(\mathbf{x}, t)]$$

### 4.3 Mean-field Model

Application of Liouville's theorem leads to a system of ordinary differential equations.

$$\dot{\mathbf{x}} = \mathbf{a}^T(\mathbf{x})$$

The immunotherapy mean-field model has three fixed points: trivial, treatment succes, co-existence. We denote the fixed points as  $\mathbf{x}_{tr}$ ,  $\mathbf{x}_{ts}$ , and  $\mathbf{x}_{co}$  respectively. We denote  $(\infty, 0)$  as  $\mathbf{x}_{\infty}$  for convenience.

$$\mathbf{x}_{tr} = (0, 0); \quad \mathbf{x}_{ts} = (0, K); \quad \mathbf{x}_{co} = \left( \frac{r_Y(r_X - K\delta)}{K\delta(\beta - \delta\chi)}, \frac{r_X}{\delta} \right)$$

The co-existence fixed point is only relevant when the X component is greater than zero as we restrict the model to the first quadrant of the real plane. That is either  $(r_X - K\delta)$  and  $(\beta - \delta\chi)$  both positive together or negative together.

Linearizing around these fixed points one-by-one

$$\mathbf{J}(\mathbf{x}_{tr}) = \begin{bmatrix} r_X & 0 \\ 0 & r_Y \end{bmatrix}$$

The eigenvalues of  $\mathbf{J}(\mathbf{x}_{tr})$  are  $r_X$  and  $r_Y$ , by definition they are always positive. Hence,  $\mathbf{x}_{tr}$  is always an unstable fixed point.

$$\mathbf{J}(\mathbf{x}_{ts}) = \begin{bmatrix} r_X - K\delta & 0 \\ (\beta - \delta\chi)K & -r_Y \end{bmatrix}$$

The eigenvalues of  $\mathbf{J}(\mathbf{x}_{ts})$  are  $(r_X - K\delta)$  and  $-r_Y$  with corresponding eigenvectors  $(\frac{r_Y + r_X - K\delta}{K(\beta - \delta\chi)}, 1)$  and  $(0, 1)$  respectively. As  $-r_Y$  is always negative  $\mathbf{x}_{ts}$  is always attracting on the y-axis. For  $(r_X - K\delta) > 0$ ,  $\mathbf{x}_{ts}$  is a saddle point and for  $(r_X - K\delta) < 0$  it is a stable fixed point.

$$\mathbf{J}(\mathbf{x}_{co}) = \begin{bmatrix} 0 & -\frac{r_Y(r_X - K\delta)}{K(\beta - \delta\chi)} \\ \frac{r_X}{\delta}(\beta - \delta\chi) & -\frac{r_X r_Y}{K\delta} \end{bmatrix}$$

The eigenvalues of  $\mathbf{J}(\mathbf{x}_{co})$  are  $\lambda_{\pm} = \frac{1}{2} \left[ -\gamma \pm \sqrt{\gamma^2 - 4\gamma(r_X - K\delta)} \right]$  where  $\gamma = \frac{r_X r_Y}{K\delta}$ . For  $(r_X - K\delta) > \frac{\gamma}{4}$ , eigenvalues are imaginary and have negative real part. For  $(r_X - K\delta) < 0$ ,  $\lambda_+$  is real and positive while  $\lambda_-$  is real and negative.

The patient dynamics can be categorized into four cases based on the behavior of fixed points in different parameter regions.

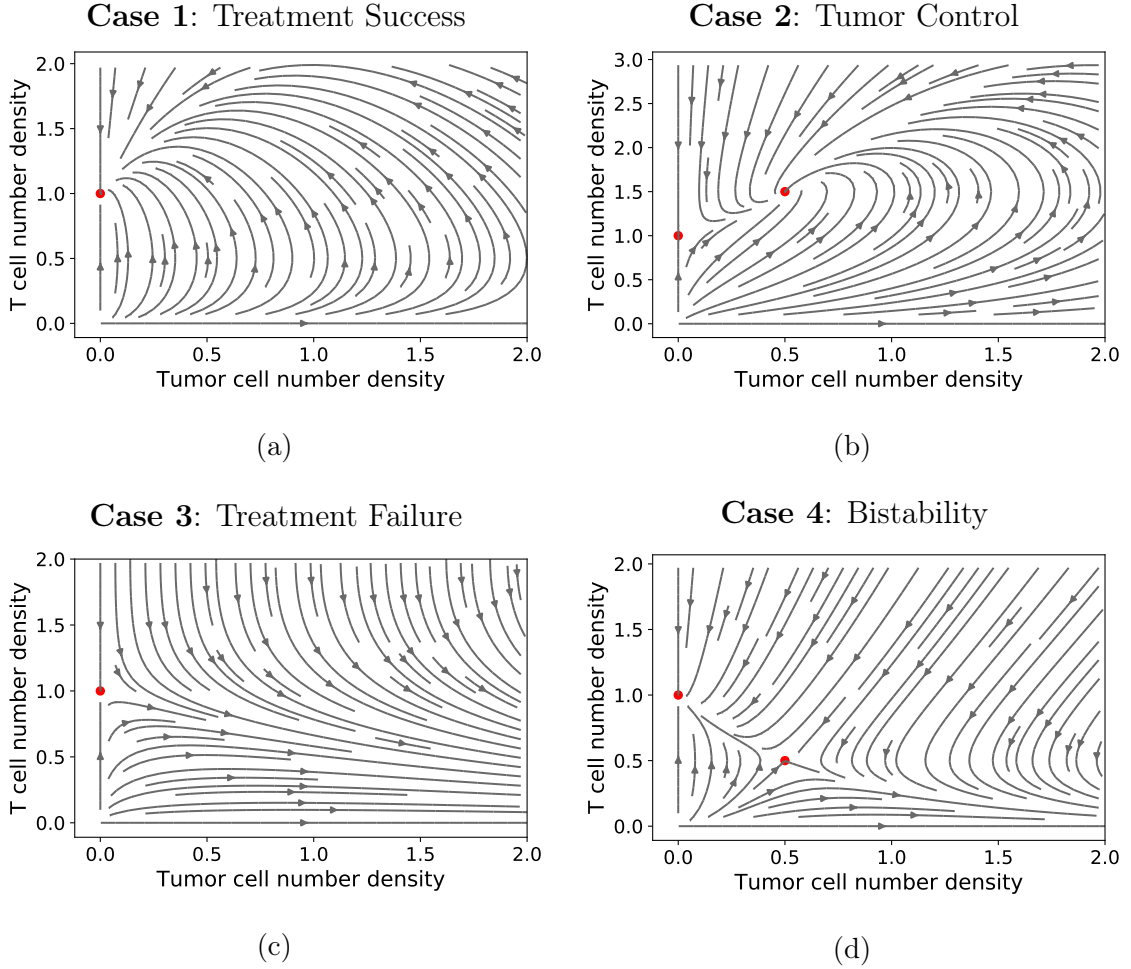


Figure 4.2: **Mean-field phase portrait of tumor cells and T cells under immunotherapy.** Panel (a) the phase space trajectories in this parameter region lead to  $\mathbf{x}_{ts}$  fixed point. Panel (b) the phase space trajectories in this parameter region converge to  $\mathbf{x}_{co}$  fixed point. Panel (c) the phase space trajectories in this parameter region diverge to  $\mathbf{x}_{\infty}$ . Panel (d) the phase space trajectories in this parameter region converge to either  $\mathbf{x}_{ts}$  or diverge to  $\mathbf{x}_{\infty}$  based on the initial conditions.

**Case 1: Treatment Success** (Figure 4.2a)  $(r_X - K\delta) < 0$  ;  $(\beta - \delta\chi) > 0$

$$r_X = 0.5, \quad r_Y = 1, \quad \beta = 2$$

When the tumor growth rate is less than the rate of killing imposed at immune carrying capacity, and the overall T cell proliferation due to effector function is positive, treatment success is observed. In this case, there is only one fixed point  $\mathbf{x}_{ts}$ , and tumor cells go extinct independent of the starting conditions.

**Case 2:** Tumor Control (Figure 4.2b)  $(r_X - K\delta) > 0$ ;  $(\beta - \delta\chi) > 0$

$$r_X = 1.5, \quad r_Y = 1, \quad \beta = 2$$

When the tumor growth rate is not less than the rate of killing imposed at immune carrying capacity, and the overall T cell proliferation due to effector function is positive, control of tumor load is observed. There are two fixed points  $\mathbf{x}_{ts}$  and  $\mathbf{x}_{co}$  that is leukemia either get cured or is maintained at an equilibrium level. The basin of attraction of  $\mathbf{x}_{ts}$  is the y-axis, and for any positive number density of tumor cells leads to  $\mathbf{x}_{co}$ .

**Case 3:** Treatment Failure (Figure 4.2c)  $(r_X - K\delta) > 0$ ;  $(\beta - \delta\chi) < 0$

$$r_X = 2, \quad r_Y = 1, \quad \beta = 0$$

When the tumor growth rate is higher than the rate of killing imposed at immune carrying capacity, and the overall T cell proliferation due to effector function is negative, treatment failure is observed. There is a fixed point  $\mathbf{x}_{ts}$  with the y-axis as the basin. Trajectories from every other initial point diverge to  $\mathbf{x}_\infty$ , that is, tumor cells do not go extinct.

**Case 4:** Bistability (Figure 4.2d)  $(r_X - K\delta) < 0$ ;  $(\beta - \delta\chi) < 0$

$$r_X = 0.5, \quad r_Y = 1, \quad \beta = 0$$

When the tumor growth rate is lower than the rate of killing imposed at immune carrying capacity, and the overall T cell proliferation due to effector function is also negative, bistability is observed in the system. There are two fixed points,  $\mathbf{x}_{ts}$  and  $\mathbf{x}_{co}$ , corresponding to the eradication of tumor cells, and coexistence with effector T cells, respectively. There is a stable manifold separating the basin of attraction of  $\mathbf{x}_{ts}$  and  $\mathbf{x}_\infty$  passing through  $\mathbf{x}_{co}$ .

## 4.4 Stochastic Model

Using the Feynmann-Kac formula (section 2.7), we can obtain the stochastic differential equations for chemotherapy.

$$\dot{\mathbf{x}} = \mathbf{a}^I(\mathbf{x}) + \sqrt{B^I(\mathbf{x})} \boldsymbol{\xi}(t)$$

Using the procedure to obtain the alternative system as directed in section 2.7 we get

$$\dot{\mathbf{x}} = \mathbf{a}^I(\mathbf{x}) + C^I(\mathbf{x}) \boldsymbol{\xi}^*(t)$$

## 4.5 First-passage Analysis

The killing of tumor cells leads to an increased contribution of random fluctuations in the dynamics. The system does not strictly follow deterministic trajectories due to fluctuations. We perform first-passage analysis for the parameters that correspond to the case of Bistability. As a proxy to exit on the  $\mathbf{x}_\infty$ , we measure exit probability on the unstable manifold at  $\mathbf{x} = (2, 0.1)$ . The probabilities of exit at  $\mathbf{x}_{ts}$ , and a point on the unstable manifold have a peculiar effect on the effective basin boundary. The line of equal probabilities of exit through either of the exit points is not on the stable manifold. This line is away from the y-axis, increasing the realized basin for the extinction of tumor cells (Figure 4.3c).

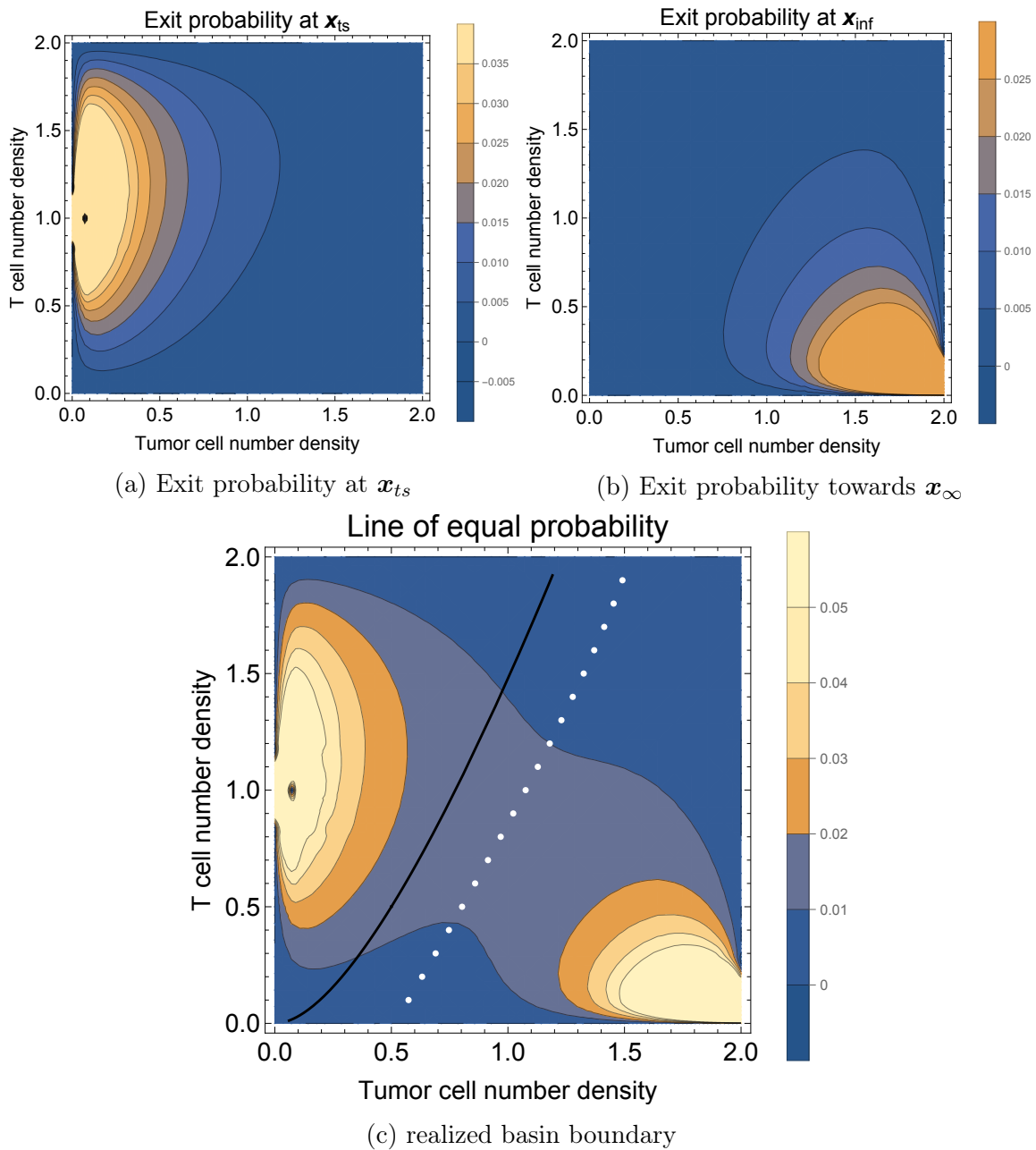


Figure 4.3: **Exit probabilities and the realized basin boundary under immunotherapy.** The extinction of tumor population can take place with some non-zero probability even if deterministically it is in different basin of attraction. The white dotted line is the line of equal probabilities of exit through either of the exit points. This line is away from the origin compared to the stable manifold, i.e. the points between stable manifold and the line of equal probability have higher chance of getting extinct compared to diverging to  $x_{\infty}$  despite being in the basin of  $x_{\infty}$ .



# Chapter 5

## Discussion

In this study, we model B lymphocyte leukemia that is known for its tendency to return. The basis of the disease relapse is correlated with the post-treatment residual disease (Della Starza et al. 2019), motivating a stochastic description. To obtain an understanding of the disease relapse, we model leukemia under contemporary treatments, chemotherapy, and immunotherapy. The treatments affect the lymphoblast populations in fundamentally different ways. The chemotherapy targets cell proliferation; hence, the faster the cells grow, the more are they affected. The leukemia populations are functionally heterogeneous, due to the mutations; proliferation is one of the ways this can surface (Hope et al. 2004). Before treatment, the fast-growing cells represent the populations; this is reversed due to chemotherapy. Since the slow cells represent the disease, the relapse followed by chemotherapy is slow.

The immunotherapy directs the adaptive immune system to kill the tumor cells using an antibody (Nagorsen and Baeuerle 2011). Blinatumomab, a bi-specific T cell engager, targets CD19, a cell surface-bound macromolecule, that is fundamental to the existence of a B lymphocyte tumor cell. As a result, killer T cells eliminate any target cells presenting the CD19 molecule, regardless of their growth rate. Hence, if slow cells and fast cells are present in the same amount, they will experience similar mortality rates. Since the proportion of slow and fast cells are the same at the end of the treatment, the relapse tends to be dominated by fast-growing cells.

There are studies by Viossat and Noble 2020, Gatenby et al. 2009 suggesting tumor containment over eradication. The eradication strategy specifies using a high dose of treatment to kill all the tumor cells. Contrary to that, the tumor containment strategy suggests maintaining the tumor below lethal levels. The latter approach is better in two ways: reduced toxicity and low chance of resistant tumor. Containing

the tumor requires less dosage of drugs, and therefore fewer adverse effects. Resistance to chemotherapy usually comes with fitness disadvantages (Gatenby and Brown 2018) and can not outgrow non-resistant cells in the absence of high selection pressure. Exploiting this type of competition, we can maintain a treatment sensitive disease under control. The proposed model of immunotherapy predicts a way to contain the tumor (Figure 4.2b) without requiring any competition. Specifically, if the immune system can be primed such that the T cell activation outweighs T cell exhaustion,  $(\beta - \delta\chi) > 0$ , the disease does not grow indefinitely (Figure 4.2a, Figure 4.2b).

For a series of coin tosses, if a particle is moved right at every occurrence of heads and moved left every tail on a line, the particle is said to follow a random walk. Far away from the starting position of the particle, if one keeps a hole, with the condition that once the particle reaches the hole, it can not continue further; this is known as the absorbing boundary for random walks. It is known that independent of the initial position after sufficient time, the particle is found in the hole. The tumor cell numbers are reduced rapidly in both types of present-day treatments. Population with small sizes fall vulnerable to random fluctuations. If the system persists in this state, the fluctuations are capable of driving the system to extinction. To show this, we draw an analogy between the state of the disease and random walk. The analysis of exit probabilities confirms that the tumor populations with a low number of cells have more chances of getting extinct stochastically (Figure 3.3, Figure 4.3).

The tumor always grows by the rate of the fastest present phenotype. Thus, if the fast cells are removed, then the net growth rate of the disease is reduced (Figure 3.2). The immunotherapy performs better for a slow-growing tumors,  $(r_X - K\delta) < 0$  (Figure 4.2a, Figure 4.2d). First, applying chemotherapy lowers the net growth rate of leukemia. It is easy to control the slow-growing tumor by applying immunotherapy. This way the tumor gets extinct by a persistent immune response (Figure 4.2a) or stochastically (Figure 4.3). The sequence of an initial block of chemotherapy followed by prolonged immunotherapy can not only contain tumors effectively but also escape the adverse effects of high dose treatments.

The master equation and the Fokker-Planck equation arise in all the fields of science. Given the rarity of analytical solutions, the only way to solve the equation is through numerical methods. However, in practice, this more often than not, demand a lot of computing power. The connection between the Fokker-Planck equation and the stochastic differential equation, the Feynmann-Kac formula, has been realized but has rarely been implemented for computations. This study illustrates an implementation of this connection and brings attention to advances in Runge-Kutta algorithms to solve the stochastic differential equation. Additionally, the alternative stochastic model

proposed with the equivalent diffusion matrix  $C$  instead of  $B$  in the section 2.7 provides more speed up in solving stochastic differential equations. It exploits the fact that computing square root of the entries of a matrix is orders of magnitude faster than computing the square root of a matrix.

The formulation of the models is in such a way that it can be used in practice right away. The input/output of the model is in terms of cell numbers or tumor load, a norm in the clinical practice. Blood counts are monitored frequently during the treatment to assess the situation; using these patient-specific trajectories of lymphocyte counts can be obtained. The reactions used in the model represent the real biological processes, and their rates can be calibrated using a time series of lymphocyte counts. Parameters related to the growth and death of cells can be calibrated by fitting patient data. The parameters related to cell interactions may require additional in vitro experiments. The workflow developed here is such that by writing chemical reactions for the system, the master equation, the Fokker-Planck equation, and the differential equations immediately follow. To conclude, we present a simple implementation of a model integrating cell interaction into a quantitative understanding of contemporary leukemia treatments. The study bridges some standard tools from statistical mechanics and economics to analyze the behavior of the disease easing the computational effort required to examine treatment strategies.



# References

- Pui, C.-H., L. L. Robison, and A. T. Look (2008). “Acute lymphoblastic leukaemia”. In: *The Lancet* 371.9617, pp. 1030–1043.
- Faderl, S., S. O’Brien, C.-H. Pui, et al. (2010). “Adult acute lymphoblastic leukemia: Concepts and strategies”. In: *Cancer* 116.5, pp. 1165–1176.
- Pui, C.-H. (2006). “Central Nervous System Disease in Acute Lymphoblastic Leukemia: Prophylaxis and Treatment”. In: *Hematology* 2006.1, pp. 142–146.
- Jabbour, E., D. Thomas, J. Cortes, H. M. Kantarjian, and S. O’Brien (2010). “Central nervous system prophylaxis in adults with acute lymphoblastic leukemia: Current and emerging therapies”. en. In: *Cancer*.
- Siegel, R. L., K. D. Miller, and A. Jemal (2015). “Cancer statistics, 2015: Cancer Statistics, 2015”. In: *CA: A Cancer Journal for Clinicians* 65.1, pp. 5–29.
- Della Starza, I., S. Chiaretti, M. S. De Propriis, et al. (2019). “Minimal Residual Disease in Acute Lymphoblastic Leukemia: Technical and Clinical Advances”. In: *Frontiers in Oncology* 9, p. 726.
- Gökbuget, N., D. Stanze, J. Beck, et al. (2012). “Outcome of relapsed adult lymphoblastic leukemia depends on response to salvage chemotherapy, prognostic factors, and performance of stem cell transplantation”. In: *Blood* 120.10, pp. 2032–2041.
- Schmiegelow, K., K. Müller, S. S. Mogensen, et al. (2017). “Non-infectious chemotherapy-associated acute toxicities during childhood acute lymphoblastic leukemia therapy”. In: *F1000Research* 6, p. 444.
- Prucker, C., C. Peters, M. N. Dworzak, et al. (2009). “Induction death and treatment-related mortality in first remission of children with acute lymphoblastic leukemia: a population-based analysis of the Austrian Berlin-Frankfurt-Münster study group”. In: *Leukemia* 23.7, pp. 1264–1269.
- Stary, J., M. Zimmermann, M. Campbell, et al. (2014). “Intensive Chemotherapy for Childhood Acute Lymphoblastic Leukemia: Results of the Randomized Intercontinental Trial ALL IC-BFM 2002”. In: *Journal of Clinical Oncology* 32.3, pp. 174–184.
- Nagorsen, D. and P. A. Baeuerle (2011). “Immunomodulatory therapy of cancer with T cell-engaging BiTE antibody blinatumomab”. In: *Experimental Cell Research* 317.9, pp. 1255–1260.

- Kantarjian, H., A. Stein, N. Gökbuget, et al. (2017). “Blinatumomab versus Chemotherapy for Advanced Acute Lymphoblastic Leukemia”. In: *New England Journal of Medicine* 376.9, pp. 836–847.
- Bassan, R., M. Brüggemann, H.-S. Radcliffe, et al. (2019). “A systematic literature review and meta-analysis of minimal residual disease as a prognostic indicator in adult B-cell acute lymphoblastic leukemia”. In: *Haematologica* 104.10, pp. 2028–2039.
- Knudson, A. G. (1971). “Mutation and Cancer: Statistical Study of Retinoblastoma”. In: *Proceedings of the National Academy of Sciences* 68.4, pp. 820–823.
- Kimmel, M. and D. E. Axelrod (1990). “Mathematical models of gene amplification with applications to cellular drug resistance and tumorigenicity”. In: *Genetics* 125.3, pp. 633–644.
- Altrock, P. M., L. L. Liu, and F. Michor (2015). “The mathematics of cancer: integrating quantitative models”. In: *Nature Reviews Cancer* 15.12, pp. 730–745.
- Michor, F., T. P. Hughes, Y. Iwasa, et al. (2005). “Dynamics of chronic myeloid leukaemia”. en. In: *Nature* 435.7046, pp. 1267–1270.
- Dingli, D., A. Traulsen, and J. M. Pacheco (2008). “Chronic Myeloid Leukemia: Origin, Development, Response to Therapy, and Relapse”. In: *Clinical Leukemia* 2.2, pp. 133–139.
- Werner, B., D. Dingli, T. Lenaerts, J. M. Pacheco, and A. Traulsen (2011). “Dynamics of Mutant Cells in Hierarchical Organized Tissues”. In: *PLoS Computational Biology* 7.12. Ed. by N. L. Komarova, e1002290.
- Komarova, N. (2006). “Stochastic modeling of drug resistance in cancer”. en. In: *Journal of Theoretical Biology* 239.3, pp. 351–366.
- Ferreira, S. C., M. L. Martins, and M. J. Vilela (2002). “Reaction-diffusion model for the growth of avascular tumor”. In: *Physical Review E* 65.2, p. 021907.
- Macklin, P., S. McDougall, A. R. A. Anderson, et al. (2009). “Multiscale modelling and nonlinear simulation of vascular tumour growth”. In: *Journal of Mathematical Biology* 58.4-5, pp. 765–798.
- Waclaw, B., I. Bozic, M. E. Pittman, et al. (2015). “A spatial model predicts that dispersal and cell turnover limit intratumour heterogeneity”. In: *Nature* 525.7568, pp. 261–264.
- Kalos, M., B. L. Levine, D. L. Porter, et al. (2011). “T Cells with Chimeric Antigen Receptors Have Potent Antitumor Effects and Can Establish Memory in Patients with Advanced Leukemia”. In: *Science Translational Medicine* 3.95, 95ra73–95ra73.
- Kimmel, G. J., F. L. Locke, and P. M. Altrock (2019). *Response to CAR T cell therapy can be explained by ecological cell dynamics and stochastic extinction events*. preprint. Cancer Biology.
- Gardiner, C. W. (2009). *Stochastic methods: a handbook for the natural and social sciences*. 4th ed. Springer series in synergetics 13. Berlin: Springer.
- Øksendal, B. (2003). *Stochastic Differential Equations*. Universitext. Berlin, Heidelberg: Springer Berlin Heidelberg.
- Denman, E. D. (1981). “Roots of real matrices”. In: *Linear Algebra and its Applications* 36, pp. 133–139.

- Björck, Å. and S. Hammarling (1983). “A Schur method for the square root of a matrix”. In: *Linear Algebra and its Applications* 52-53, pp. 127–140.
- Allen, E. (2007). *Modeling with Itô Stochastic Differential Equations*. Vol. 22. Mathematical Modelling: Theory and Applications. Dordrecht: Springer Netherlands.
- Gillespie, D. T. (1977). “Exact stochastic simulation of coupled chemical reactions”. In: *The Journal of Physical Chemistry* 81.25, pp. 2340–2361.
- Kloeden, P. E. and E. Platen (1992). *Numerical Solution of Stochastic Differential Equations*. Berlin, Heidelberg: Springer Berlin Heidelberg.
- Rößler, A. (2009). “Second Order Runge–Kutta Methods for Itô Stochastic Differential Equations”. In: *SIAM Journal on Numerical Analysis* 47.3, pp. 1713–1738.
- Aburn, M. (2015). *sdeint*.
- Oliphant, T. E. (2007). “Python for Scientific Computing”. In: *Computing in Science & Engineering* 9.3, pp. 10–20.
- Millman, J. K. and M. Aivazis (2011). “Python for Scientists and Engineers”. In: *Computing in Science & Engineering* 13.2, pp. 9–12.
- Hunter, J. D. (2007). “Matplotlib: A 2D Graphics Environment”. In: *Computing in Science & Engineering* 9.3, pp. 90–95.
- Meurer, A., C. P. Smith, M. Paprocki, et al. (2017). “SymPy: symbolic computing in Python”. In: *PeerJ Computer Science* 3, e103.
- Walt, S. van der, C. S. Colbert, and G. Varoquaux (2011). “The NumPy Array: A Structure for Efficient Numerical Computation”. In: *Computing in Science & Engineering* 13.2, pp. 22–30.
- Hope, K. J., L. Jin, and J. E. Dick (2004). “Acute myeloid leukemia originates from a hierarchy of leukemic stem cell classes that differ in self-renewal capacity”. In: *Nature Immunology* 5.7, pp. 738–743.
- Viossat, Y. and R. Noble (2020). *The logic of containing tumors*. preprint. Cancer Biology.
- Gatenby, R., A. S. Silva, R. J. Gillies, and B. R. Frieden (2009). “Adaptive Therapy”. In: *Cancer Research* 69.11, pp. 4894–4903.
- Gatenby, R. and J. Brown (2018). “The Evolution and Ecology of Resistance in Cancer Therapy”. In: *Cold Spring Harbor Perspectives in Medicine* 8.3, a033415.